Investigation on the Thermo-Mechanical Behavior of an Energy Pile and the Surrounding Soil by Model Test and 2D Finite Element-Finite Difference Method

X. H. Bao[1(✉)], Y. L. Xiong[2], H. Y. Mingi[1], H. Z. Cui[1], G. B. Liu[2], and R. Y. Zheng[2]

[1] Shenzhen University, Shenzhen 518060, China
bxh@szu.edu.cn
[2] Ningbo University, Ningbo 315211, China

Abstract. The exploitation of geothermal energy could cause additional thermal load imposed to the foundation and surrounding soils. The effects of temperature changes on the response of energy piles which can induce thermal expansion and contraction of both piles and soils need to be examined. This study investigated the behaviors of an energy pile and the surrounding soil using the model test and 2D thermo-hydro-mechanical finite element-finite difference (FE-FD) method that can solve soil-water-temperature coupling problems based on three phase field theory. In the numerical analysis, the thermo-mechanical property of soil could be described by a new thermo-elastoplastic constitutive model, in which, the concept of equivalent thermal stress was adopted. Time change of temperature and displacement of the pile and soil, axial stress of pile are investigated. The simulated results are in good agreement with those obtained from the laboratory test on a model energy pile. Attention is dedicated to the development of pore water pressure that could cause thermo-consolidation of soil and bring the settlement of pile-soil system. In some circumstances, long-term instability of the pile-soil might happen through years of heating and cooling cycles.

Keywords: Energy piles · THM · Model test · FE-FD method

1 Introduction

The use of sustainable geothermal energy has significant meaning in saving of conventional energy sources and protecting the environment. The energy pile, also referred to as heat exchange pile, is an innovative and sustainable foundation solution because of its dual function of supporting superstructure load and harvesting geothermal energy. The performance of the energy pile is based on absorbing and injecting heat in ground and this kind of heat transfer in the energy pile can result in temperature variation in the pile and surrounding soil, which cause pile and soil to expand and contract, further affect the bearing capacity of pile or cause thermo-consolidation of soil, then influence the foundation and structure resistance.

Within the past decade, energy piles have been used in many large construction projects, however, most of the energy pile design is still based on experience and empirical methods derived from field tests (Gao et al. 2008; Katsura et al. 2009; Jalaluddin et al. 2011; Loveridge et al. 2013). Most of these studies focused on the heat transfer behavior of the energy pile system, some also focus on the thermo-mechanical behavior of piles influenced by temperature changes (Laloui et al. 2006; Bourne-Webb et al. 2009; Olgun et al. 2012; Murphy et al. 2014). Except for the field tests, laboratory model tests including material tests for energy piles (Wang et al. 2011; Stewart and McCartney 2014; Yavari et al. 2014; Kramer et al. 2015; Marto and Amaludin 2015; Bao et al. 2017; Yang et al. 2017) and numerical analysis (Ghasemi-Fare and Basu 2015; Saggu and Chakraborty 2015; Di Donna et al. 2016; Caulk et al. 2016) are also performed to investigate thermo-mechanical behavior of the energy pile, particularly the composite energy pile or under different thermo-load conditions. However, in most of the numerical models, a fairly simple method was used for calculating the thermo-mechanical behavior of pile and soil system. The models were unable to analysis the effect of thermo-consolidation and thermo-plastic property of soil which is of importance for considering soil-pile interaction behavior, especially the saturated clay that temperature change may cause large pore water pressure, and then lead to large amount of settlement of the ground and pile under long-term cyclic heating-cooling cycles.

Full-scale pile heating tests in field can help in understanding the thermal and mechanical performance of piles. However, large-scale laboratory tests on model piles can be advantageous over full-scale pile heating tests because of the high cost and uncertain field conditions associated with field tests. Moreover, soil properties can be controlled and measured more easily in laboratory than in the field. Thus, as pointed out by Kramer et al. (2015), results from controlled laboratory tests can be helpful in providing meaningful insight into the physics of a complex process and the tests results can be used to verify predictions from numerical analysis of energy piles, as presented in this paper.

Therefore, in the present study, using the finite element-finite difference (FE-FD) method, the thermo-mechanical behavior of a large model-scale energy pile with an embedded U tube was investigated. The model pile was installed in saturated clay prepared through compaction layer by layer. In the simulation, the thermo-mechanical property of the saturated clay was described using a new thermo-elastoplastic constitutive model, in which, the concept of equivalent thermal stress was adopted and the mechanical behavior of soil including structure, overconsolidation and anisotropy at different temperature states could be described in a unified way. Time change of temperatures and displacements of the pile and soil are investigated. Attention is dedicated to the development of pore water pressure which could cause thermo-consolidation of soil. The calculated results are in good agreement with those obtained from the laboratory test.

2 FE-FD Method

2.1 Basic Theory

The problem is presented by a reinforced concrete model pile which is subjected to vertical mechanical loads and exchanges heat with the surrounding soil at the same time. The soil is considered as porous material, composed of solid phase and fluid

phase and the entire medium is considered to be fully saturated by water. Thus, the study is a typical thermal-hydraulic-mechanical (THM) problem, that mechanical, thermal and hydraulic are fully coupled because the volume change of the materials is effected by temperature. Moreover, the heat exchange between pile and soil depends on the pore water flow and the mechanical response of soil also depends on the pore water pressure. Therefore, a fully coupled thermo-hydro-mechanical formulation is needed for the numerical simulation.

In this study, a finite element-finite difference (FE-FD) theory proposed by Oka et al. (1994) was adopted to formulate the THM coupling equations which were incorporated in the software SOFT and then numerical simulation could be performed using the program SOFT. In this program, the equilibrium equation and energy conservation equation were discretized by FEM, while the continuity equation was discretized by backward FDM. The displacement, pore water pressure and temperature were taken as the variables in the field equations as shown in the following:

(1) Equilibrium equation:

$$\rho \ddot{u}_i^s = \frac{\partial \sigma_{ij}}{\partial x_j} + \rho b_i \tag{1}$$

(2) Continuity equation for soil-water:

$$\frac{\dot{\varepsilon}_{ii}^s}{n} - \frac{k}{\gamma_w} \frac{\partial^2 P_d}{\partial x_i \partial x_i} - \frac{\dot{P}_d}{K^w} - 3\alpha_t^w \dot{T} = 0 \tag{2}$$

(3) Energy equation:

$$\rho c \frac{\partial T}{\partial t} + n(\rho c)^w v_i \frac{\partial T}{\partial x_i} = k_t \frac{\partial^2 T}{\partial x_i \partial x_i} + Q \tag{3}$$

Where, ρ is the bulk density of the porous material including soil particles and water, $\bar{\rho}^s = (1 - n)\rho^s$ is the apparent density of solid, $\bar{\rho}^w = n\rho^w$ is the apparent density of water $(\rho = \bar{\rho}^s + \bar{\rho}^w = (1 - n)\rho^s + n\rho^w)$, n is the porosity, u^s is the displacement vectors of solid and water respectively, σ_{ij} is the stress tensor, b_i is the body force, w_i is the relative displacement vector between liquid and solid phases, ε_{ij}^s is the strain tensor of solid, k is the soil permeability, P_d is the excess pore water pressure, K^w is the bulk modulus of water, α_t^w is the linear thermal expansion coefficient of water, c is the specific heat of soil including solid and water $(\rho c = (1 - n)(\rho c)^s + n(\rho c)^w)$, k_t is the average heat conductivity including solid and water $\left(k_t = (1 - n)k_t^s + nk_t^w\right)$, v_i is the velocity of fluid, T is the temperature and Q is energy produced by the heat source per unit volume.

After discretization, the final THM FE-FD field equation can be obtained as:

$$
\begin{bmatrix} [K] & \vec{K}_v \\ \vec{K}_v^T & -(\bar{A}+\bar{\alpha}) \end{bmatrix} \left\{ \begin{array}{c} \Delta\vec{u}_N|_{t+\Delta t} \\ h_{|t+\Delta t} \end{array} \right\} + \left\{ \begin{array}{c} 0 \\ \sum_{i=1}^{m} \bar{\alpha}_i h_{i|t+\Delta t} \end{array} \right\}
$$

$$
= \left\{ \begin{array}{c} \Delta\vec{F}_{|t+\Delta t} + \Delta\vec{F}_{|Rt+\Delta t} + \vec{K}_v h_{|t} + \vec{F}_T \Delta\vec{T}_{N|t+\Delta t} \\ \left[\vec{K}_{vT}\right]\Delta\vec{T}_{N|t+\Delta t} - \bar{A}h_{|t} \end{array} \right\} \left([C^t] + \bar{\beta}\Delta t[K^t]\right)\dot{\vec{T}}_{N|t+\Delta t} \qquad (4)
$$

$$
= [F^t] - [K^t]\left(\vec{T}_{N|t} + (1-\bar{\beta})\Delta t\dot{\vec{T}}_{N|t}\right)
$$

The detailed information about the field equation can be seen in the reference (Xiong et al. 2014).

2.2 Thermo-Elastoplastic Constitutive Model

In the numerical simulation, the behavior of the reinforced concrete is considered thermo elastic, whereas the soil behavior should be described by thermo-elastoplastic constitutive model. The temperature change can cause elastic and plastic volumetric strain, which is similar to the behavior that the stress performances, so the concept of "equivalent stress" is introduced. The similarity of volumetric strain caused by real stress and equivalent stress due to temperature change was clearly described in the work by Xiong et al. (2016). According to the Hooke's law, the equivalent stress $\Delta\tilde{\sigma}_{ij}$ can be expressed as:

$$
\Delta\tilde{\sigma}_{ij} = 3K\alpha_T(T-T_0)\delta_{ij} \qquad (5)
$$

Where, K is the bulk modulus of the soil, α_T is the linear thermal expansion coefficient, T is the actual temperature and T_0 is the reference temperature (usually assumed to be 15 °C).

The result that the change of temperature can cause elastic and plastic volumetric strain was confirmed by experimental date (Eriksson 1989). Therefore, based on the elastoplastic constitutive model at normal temperature condition (Zhang et al. 2011, 2012), the thermo-elastoplastic constitutive model can be obtained by changing overconsolidation state variable R to temperature state variable $\tilde{R}$. The yield function adopted in the model is the function of the modified Cam-clay model considering the overconsolidation, structure and saturation of clay soil, which can be written as:

$$
f = \ln\frac{p}{p_0^*} + \ln\frac{M^2 - \varsigma^2 + \eta^{*2}}{M^2 - \varsigma^2} + \ln R^* - \ln R - \frac{\rho_s}{1+e_0}\frac{1}{C_p} - \frac{\varepsilon_v^p}{C_p} = 0 \qquad (6)
$$

Where,

$$C_p = \frac{\lambda - \kappa}{1 + e_0}, \qquad \eta^* = \sqrt{\frac{3}{2} \hat{\eta}_{ij} \hat{\eta}_{ij}}, \qquad \eta = \sqrt{\frac{3}{2} \eta_{ij} \eta_{ij}}, \qquad \varsigma = \sqrt{\frac{3}{2} \beta_{ij} \beta_{ij}},$$

$$\hat{\eta}_{ij} = \eta_{ij} - \beta_{ij}, \qquad \eta_{ij} = \frac{S_{ij}}{\sigma_m} \qquad \eta^{*2} = \frac{3}{2} \hat{\eta}_{ij} \hat{\eta}_{ij} = \frac{3}{2} \left(\frac{S_{ij}}{\sigma_m} - \beta_{ij} \right) \left(\frac{S_{ij}}{\sigma_m} - \beta_{ij} \right)$$

η is the stress ratio q/p in $p-q$ space q/p, ζ is the anisotropy parameter, β is the anisotropy stress tensor, M is the critical state line ratio of the normally consolidated soil.

Based on the consistency law, Eq. (5) can be written as:

$$
\begin{aligned}
df &= 0 \\
&\Rightarrow \frac{\partial f}{\partial \sigma_{ij}} d\sigma_{ij} + \frac{\partial f}{\partial \beta_{ij}} d\beta_{ij} + \frac{1}{R^*} dR^* - \frac{1}{R} dR - \frac{d\rho_s}{1 + e_0} \frac{1}{C_p} - \frac{1}{C_p} d\varepsilon_v^p = 0
\end{aligned}
\tag{7}
$$

Associated flow rule is adopted, the increment of plastic strain tensor can be obtained as:

$$d\varepsilon_{ij}^p = \Lambda \frac{\partial f}{\partial \sigma_{ij}} \tag{8}$$

$$\Lambda = \frac{\frac{\partial f}{\partial \sigma_{ij}} E_{ijkl} d\varepsilon_{kl} + \frac{Q}{C_p} \frac{1}{1 + e_0} dS_r}{h_p + \frac{\partial f}{\partial \sigma_{ij}} E_{ijkl} \frac{\partial f}{\partial \sigma_{kl}}} \tag{9}$$

Where,

$$h_p = \frac{1}{C_p (M^2 - \zeta^2 + \eta^{*2}) \sigma_m} [M_s^2 - \eta^2] \tag{10}$$

The loading criteria is given as:

$$\begin{cases} \Lambda > 0 & loading \\ \Lambda = 0 & neutral \\ \Lambda < 0 & unloading \end{cases} \tag{11}$$

The detailed explanation about the deviation of the constitutive model can be found in the reference (Xiong et al. 2016).

2.3   Material Parameters

The parameters of clay and pile used in the constitutive model are listed in Table 1. For the initial constitutive model parameters of clay and concrete, most of the parameters were obtained by laboratory tests, except for the overconsolidation, structure and anisotropy parameters which are decided according to the references (Bao et al. 2016; Ye and Ye 2016). The initial thermal property parameters of clay and concrete related to thermal properties as shown in Table 2 are also obtained from laboratory thermal tests.

Table 1. Constitutive model parameters of soil and concrete pile used in calculation.

Parameters	Clay	Concrete
Compression index λ	0.25	Null
Swelling index κ	0.06	Null
Critical state parameter M	0.82	Null
Void ratio N ($p' = 98$ kPa on $N.C.L.$)	2.4	Null
Poisson's ratio v	0.35	0.2
Over consolidation parameter m	2.2	Null
Structure parameter a	0.06	Null
Anisotropy parameter b_r	0.1	Null
Gravity γ (kN/m^3)	18	24
Permeability (m/s)	$2.3 * 10^{-7}$	$1.0 * 10^{-9}$
Elastic module E (GPa)	Null	30

Table 2. Thermal properties of soil and concrete pile used in calculation.

Parameters	Clay	Concrete
Thermal expansion coefficient α (1/K)	$5.0 * 10^{-6}$	$1.1 * 10^{-5}$
Thermal conductivity k (W/m/K)	1.51	2.94
Specific heat c (kJ/kg/K)	1.52	0.96
Specific heat of water c^w (kJ/kg/K)	4.184	

3 Test Description and Numerical Model

3.1 Test Description

The laboratory test was conducted in Ningbo University (Ningbo, China) and the schematic profile is shown in Fig. 1. The model concrete pile which was precast has a total length of 1.25 m and diameter of 0.2 m, in which a heat exchange U tube was set. The lengths of the pile and tube that buried in clay were 1 m and 0.95 m respectively. The pile was made by concrete with the strength of C30, and reinforced by 4 HRB335 type steel with diameter of 10 mm. In the present numerical simulation, the pile was assumed to be concrete material and the steel was not considered.

In this experiment, the initial temperature of the soil and pile was set to 28 °C (room temperature in summer), and then the pile was heated by keeping inlet water temperature in The U tube in a constant value of 50 °C. The heat gradually diffuses from the tube to pile and soil, when the adjacent pile soil temperature differences is less than 10%, the heat exchange can be considered stable. Keep the stable state until the excess pore water pressure fully dissipated in the soil, and then stop heating so that the temperature of pile and soil naturally returned to the room temperature of 28 °C. The effect of temperature change on the working performance of heat exchange pile can be studied in this heating-cooling cycle.

Temperature measurements were placed at several locations within soil (T1, T2, T3, T4, T5) and on pile surface (T6) to characterize the temperature evolution in soil
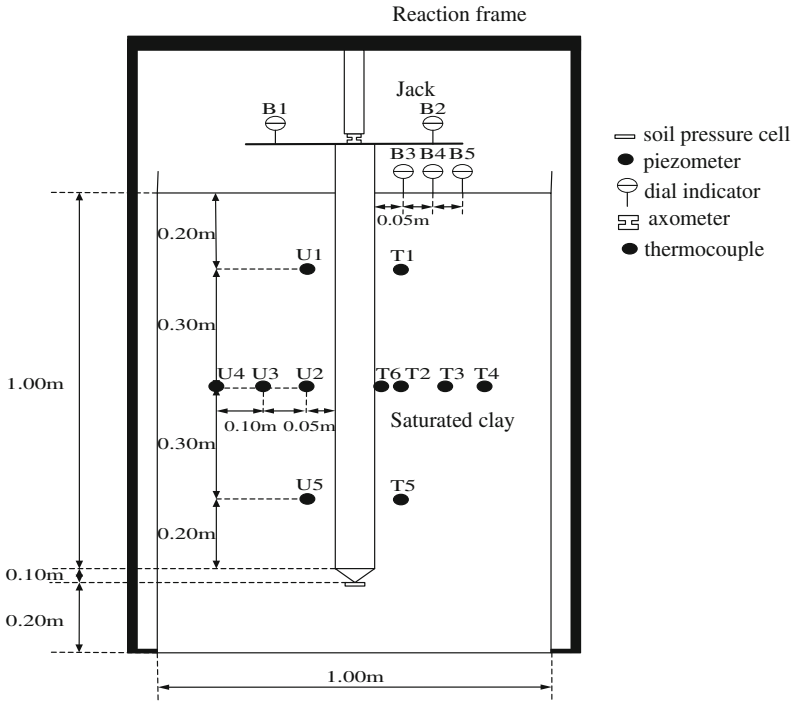
Fig. 1. Schematic diagram of pile and soil.

surrounding the pile with time change. Pore pressure measurements were also placed at several locations within soil (U1, U2, U3, U4, U5) to investigate the influence of temperature on soil behavior. Moreover, several dial indicators were placed on top of pile (B1, B2) and soil surface near pile (B3, B4, B5) to measure the displacement of pile and soil caused by temperature change. The exact locations of these instruments are clearly shown in Fig. 1.

3.2 Numerical Model

The FE-FD analysis was performed to simulate the laboratory test of the energy pile under the same conditions as those in the test. A constant inlet flow temperature $T_{inlet} =$ 50 °C of the circulation fluid at the inlet point was set. According to the laboratory test model and symmetry properties of pile and soil, the 2-D half domain of the numerical model is shown in Fig. 2, in which the red part represents the heater tube with inlet fluid and the blue part represents half of the model pile. All the size is the same as that in the laboratory test. Only the inlet flow was considered and modeled as a heat pipe with the size of 0.95 m × 0.02 m according to the tube size in the laboratory test. The thermal loading of the pile is numerically reproduced by imposing temperature paths on all of the nodes of the elements that characterize the heat pipe mesh in pile body.
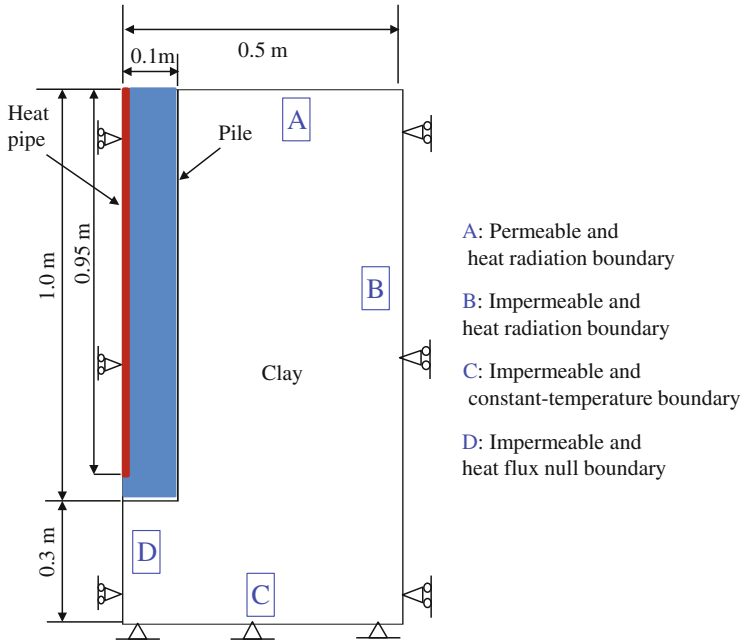
Fig. 2. Numerical model for the FE-FD analysis.

For the boundary conditions, the initial boundary condition was set according to the test condition that the vertical boundaries at the two sides have been restrained in horizontal direction and the bottom soil boundary has been restrained in both vertical and horizontal direction. As the clay was saturated, so the top soil boundary is assumed to be permeable, while the bottom boundary, left vertical soil boundary and right side boundary are impermeable. The pile is also assumed to be impermeable. The thermal boundary conditions applied in the model were heat radiation through top and right side boundaries, constant-temperature at the bottom boundary. Heat flux is assumed to be zero along the axis of symmetry of pile and soil. This method of setting of thermal boundary conditions used in FE method can be founded in references (Ghasemi-Fare and Basu 2015; Saggu and Chakraborty 2015; Di Donna et al. 2016; Caulk et al. 2016). For the initial thermal condition, the initial temperature of pile and soil was set the same as in the model tests measured before heating with a value of 28 °C, and the initial inlet flow temperature was also set he same as in test condition T_{inlet} = 50 °C.

The interface between the pile and soil surface has been modeled as frictional contact in tangential direction with a coefficient friction tan φ (φ is the internal friction angle of clay). In another word, pile-soil interface is modeled by a thin layer of element that soil and pile can slide relatively, and the pile-soil interface parameters are the same as those assumed for the soil. At the bottom of the pile soil surface, hard contact with zero penetration has been considered.

4   Comparison of Results from Numerical Simulation and Laboratory Test

This section compares the numerical results with the laboratory test results conducted in Ningbo University (Ningbo, China). As the entire test data were available to the numerical model, the numerical simulation is considered suitable for reproducing the response of the thermo-mechanical behavior of pile and soil in the heating and naturally cooling circle.

4.1   Temperature Distribution

The time-temperature curves of the points T1 (0.2 m below soil surface), T2 (0.5 m below soil surface) and T5 (0.8 m below soil surface) along the depth direction near pile (0.05 m away from pile side) are shown in Fig. 3(a). It can be seen from the figure that it took about 50 h for the thermal transfer from pile to soil and the heat exchange reached the stable state. The maximum temperature of the soil near pile side is 45.2 °C, 40.3 °C and 36.7 °C at depth of 0.2 m (T1) 0.5 m (T2) and 0.8 m (T5) below the soil surface. At the same time and the same distance of 0.05 m from the pile side, along the pile depth direction, the greater the depth of the soil, the smaller the temperature rose. The test and simulated results showed almost the same values. In Fig. 3(b), it can be seen that when the heat exchange reached the stable state, at the points 0.05 m below the soil surface, the temperatures of the soil at the distance of 0.05 m (T2), 0.15 m (T3), 0. 25 m (T4) from the pile side and on the pile surface (T6) are 40.2 °C, 35.3 °C, 32.1 °C and 45.0 °C, respectively. It is clear that at the same time, soil temperature decreased with the increase of horizontal distance from the pile side. The simulated results are in good agreement with the laboratory test results. When the heat exchange reached the stable state, the simulated temperature distribution of pile-soil is shown in Fig. 4. When the thermal cycle reached stable state, the maximum temperature in the upper part of the pile, reaching 49.7 °C, the temperature gradually reduced along the pile from top to bottom.
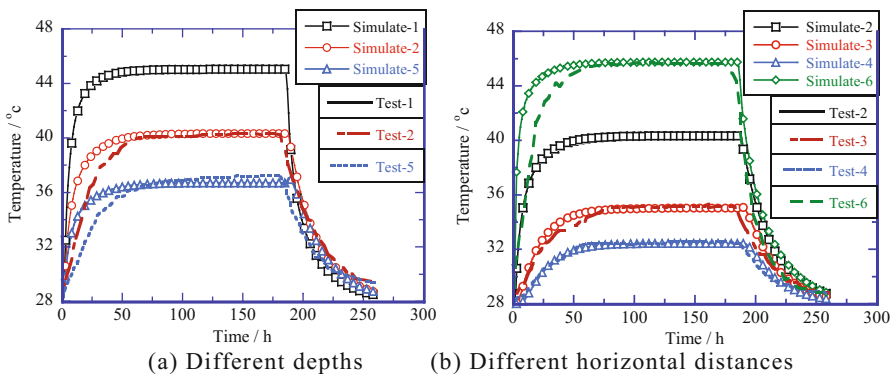

(a) Different depths   (b) Different horizontal distances

Fig. 3. Time-temperature curves of soil at different depths and horizontal distances.
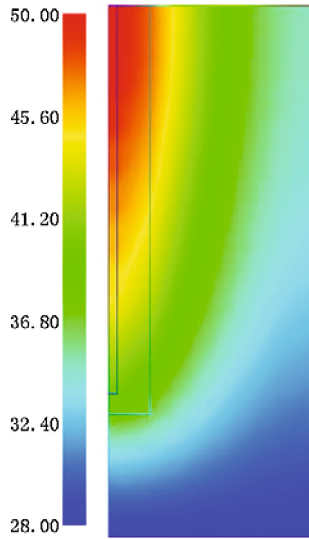
Fig. 4. Simulated distribution of temperature in pile and soil (unit: °C).

4.2 Pore Pressure in Soil

The time-excess pore water pressure (EPWP) curves at points U1 (0.2 m below soil surface), U2 (0.5 m below soil surface) and U3 (0.8 m below soil surface) 0.05 m away from the pile side are presented in Fig. 5(a). The test and simulated results showed almost the same values. It can be seen from Fig. 5(a) that the pore pressure increased sharply with the increase of temperature, and the maximum pore pressure at the points U1, U2 and U5 reached 0.70 kPa, 2.69 kPa and 4.54 kPa respectively and then slowly dissipated to the stable state. At the same time and the same distance from the pile side, the greater the depth, the higher the soil pressure caused by the
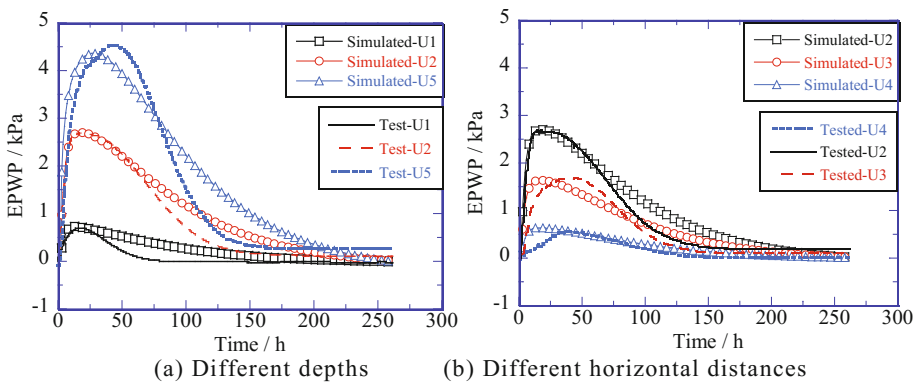

(a) Different depths   (b) Different horizontal distances

Fig. 5. Time-pore pressure curves of soil at different depths and horizontal distances.

temperature, and the longer time before the pore pressure to reach the peak value. Figure 5(b) presents the time-EPWP curves at different horizontal distance away from pile side 0.5 m below the soil surface. It can be seen from the figure that the maximum value of EPWP at points U2 (0.05 m away from pile side), U3 (0.15 m away from pile side) and U4 (0.25 m away from pile side) reached 2.69 kPa, 1.69 kPa and 0.56 kPa, respectively, and then slowly dissipated to the stable state. At the same time and the same depth, the closer to the pile side, the higher the EPWP caused by the temperature change, and the shorter the time required for the EPWP to reach the peak values. The numerical simulation results are in good agreement with the laboratory test results.

4.3 Displacement

For the sign conventions, upward displacements are considered to be positive while downward displacements are considered to be negative. Figure 6(a) shows the variation of the vertical displacement at the pile top under the heating-cooling cycle. In the heating stage, the pile uplift due to thermal expansion and arrived at the peak value at the end of heating, which means that the effect of temperature could reduce the settlement of the pile under the condition of pure heating cycle. After heating, the vertical displacement at the pile top dropped quickly. During the naturally cooling stage, the pile-soil expansion disappeared and the downward displacements increased. When arrived at the stable state, the total settlement of the pile reduced 0.16 mm, indicating that the unrecoverable plastic deformation occurred. The simulated value is slightly larger than the test value at the thermal expansion stage and slightly smaller than the total settlement value from the test. However the overall tendency is consistent with test results.

Figure 6(b) shows the variation of the vertical displacement at soil surface 0.05 m away from the pile side under the heating-cooling cycle. The simulated results and test results showed the same tendency. In the early stage of heating, the test value and simulated value of the surface uplift showed a rapid increase, and the rate of simulated uplift was faster than that of the test. When the temperature of pile and soil reached the stable state, consolidation settlement began to accumulate and soil settlement become large quickly in the naturally cooling cycle. It is clear that unrecoverable plastic deformation of soil occurs and the total settlement is about 0.25 mm when the soil-pile recovered to the initial room temperature of 28 °C. In another word, the thermo-consolidation occurred when the pore water dissipated. On the whole, the simulation results fit the test value quite well. For the displacements of pile and soil, the trends and the maximum values are comparable between the simulation and the test, while there is a significant difference in the computing time. In another word, the rate of simulated deformation is faster than that of the test. This phenomenon might be the following reasons:

(1) The permeability of soil. In test, soil permeability changed with the temperature change and the development of pore water pressure. However, in the simulation, the permeability value of soil kept constant as the initial value obtained from laboratory test.

(2) Constitutive model of soil. The thermo-elastoplastic constitutive model did not consider the creep behavior of clay that the deformation kept developing slowly for a long time after the change of loading and temperature condition. However, the used constitutive model just considered the elastic and plastic deformation in the loading and temperature change processes.
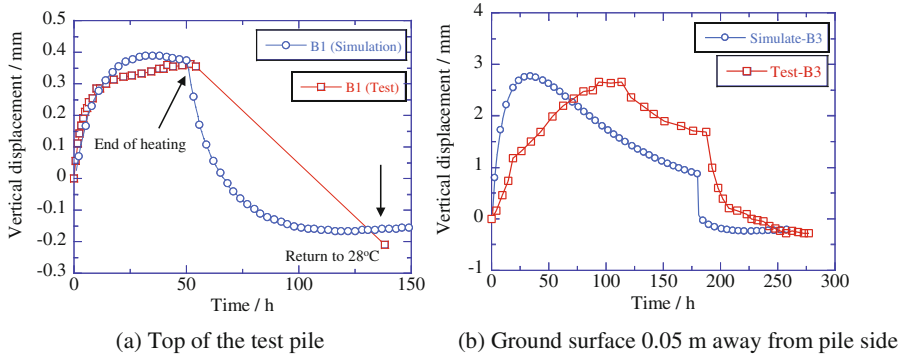

(a) Top of the test pile   (b) Ground surface 0.05 m away from pile side

Fig. 6. Time-vertical displacement curves at different places.

5   Conclusions

This study comprised both the model test and 2-D numerical simulation of the thermo-hydro-mechanical (THM) behavior of an energy pile embedded in saturated clay subjected to the heating-cooling cycle. In the used THM coupled FE-FD method, a thermo-elastoplastic constitutive model based on the concept of thermal equivalent stress was used to describe the thermo-plastic behavior of soil. The simulation results are in good agreement with the laboratory model test results, and the following conclusions can be drawn.

(1) It took about 50 h for the thermal transfer from pile to soil and the heat exchange reached the stable state when the maximum temperature appeared in the upper part of the pile. The greater the depth of the soil, the smaller the temperature rose. In another hand, soil temperature decreased with the increase of horizontal distance from the pile side.

(2) For the excess pore pressure, the greater the depth, the higher the soil pressure caused by the temperature, and the longer time required for the pore pressure to reach the peak value after the heat exchange reached the stable state. In another hand, the closer to the pile side, the higher the EPWP caused by the temperature change, and the shorter the time required for the EPWP to reach the peak value.

(3) The effect of temperature could reduce the settlement of the pile under the condition of pure heating cycle, while during the naturally cooling stage, the pile-soil expansion disappeared and the downward displacements increased indicating that the unrecoverable plastic deformation occurred.

(4) In the early stage of heating, the surface uplift showed a rapid increase, however, after the heat exchange reached the stable state, consolidation settlement began to accumulate and soil settlement become large quickly in the naturally cooling cycle indicating that the thermo-consolidation occurred due to the dissipation of pore water.

References

Bao, X., Memon, S., Yang, H., et al.: Thermal properties of cement-based composites for geothermal energy applications. Materials **10**(5), 462 (2017)

Bao, X., Ye, B., Ye, G., Zhang, F.: Co-seismic and post-seismic behavior of a wall type breakwater on a natural ground composed of liquefiable layer. Nat. Hazards **83**(3), 1799–1819 (2016)

Bourne-Webb, P., Amatya, B., Soga, K., et al.: Energy pile test at Lambeth College, London; geotechnical and thermodynamic aspects of pile response to heat cycles. Géotechnique **59**(3), 237–248 (2009)

Caulk, R., Ghazanfari, E., McCartney, J.: Parameterization of a calibrated geothermal energy pile mode. Geomech. Energy Environ. **5**, 1–15 (2016)

Di Donna, A., Rotta Loria, A., Laloui, L.: Numerical study of the response of a group of energy piles under different combinations of thermo-mechanical loads. Comput. Geotech. **72**, 126–142 (2016)

Eriksson, L.: Temperature effects on consolidation properties of sulphide clays. In: 12th International conference on soil mechanics and foundation engineering, Rio de Janeiro, pp. 2087–2090. Taylor and Francis, London, UK (1989)

Ghasemi-Fare, O., Basu, P.: Thermal operation of geothermal piles installed in sand - a comparative assessment using numerical and physical models. In: IFCEE 2015 ASCE, pp. 1721–1730 (2015)

Gao, J., Zhang, X., Liu, J., Li, K., Yang, J.: Thermal performance and ground temperature of vertical pile-foundation heat exchangers: a case study. Appl. Therm. Eng. **28**(17–18), 2295–2304 (2008)

Jalaluddin, A., Tsubaki, K., Inoue, S., Yoshida, K.: Experimental study of several types of ground heat exchanger using a steel pile foundation. Renew. Energy **36**, 764–771 (2011)

Katsura, T., Nakamura, Y., Okawada, T., Hori, S., Nagano, K.: Field test on heat extraction or injection performance of energy piles and its application. In: The 11th International Conference on Energy Storage (Effstcok2009), p. 146 (2009)

Kramer, C., Ghasemi-Fare, O., Basu, P.: Laboratory Thermal performance tests on a model heat exchanger pile in sand. Geotech. Geol. Eng. **33**, 253–271 (2015)

Loveridge, F., Holmes, G., Powrie, W., Roberts, T.: Thermal response testing through the chalk aquifer. ICE Proc. Geotech. Eng. **166**(2), 197–210 (2013)

Laloui, L., Nuth, M., Vulliet, L.: Experimental and numerical investigations of the behavior of a heat exchanger pile. Int. J. Numer. Anal. Meth. Geomech. **30**, 763–781 (2006)

Murphy, K., McCartney, J., Henry, K.: Thermo-mechanical characterization of full-scale energy foundations. In: Proceedings of the GeoCongress, ASCE, pp. 617–628 (2014)

Marto, A., Amaludin, A.: Response of shallow geothermal energy pile from laboratory model tests. In: International Symposium on Geohazards and Geomechanics (ISGG2015) IOP Conference Series on Earth and Environmental Science, vol. 26, p. 012038 (2015)

Oka, F., Yashima, A., Shimata, T., Shibata, T., Kato, M., Uzuoka, R.: FEM-FDM coupled liquefaction analysis of a porous soils using an elasto-plastic model. Appl. Sci. Res. **52**, 209–245 (1994)

Olgun, G., Martin, J., Abdelaziz, S., et al.: Field testing of energy piles at Virginia Tech. In: Proceedings of the 37th Annual Conference on Deep Foundations, Houston, TX, USA (2012)

Saggu, R., Chakraborty, T.: Cyclic thermo-mechanical analysis of energy piles in sand. Geotech. Geol. Eng. **33**, 312–342 (2015)

Stewart, M., McCartney, J.: Centrifuge modeling of soil structure interaction in energy foundations. J. Geotech. Geoenviron. Eng. **140**(4), 04013044 (2014)

Wang, B., Bouazza, A., Haberfield, C.: Preliminary observations from laboratory scale model geothermal pile subjected to thermo-mechanical loading. In: Geo-Frontiers, pp, 430–439 (2011)

Xiong, Y., Ye, G., Zhu, H., Zhang, S., Zhang, F.: Thermo-elastoplastic constitutive model for unsaturated soils. Acta Geotech. **11**, 1287–1302 (2016)

Xiong, Y., Zhang, S., Ye, G., Zhang, F.: Modification of thermo-elasto-viscoplastic model for soft rock and its application to THM analysis of heating tests. Soils Found. **54**(2), 176–196 (2014)

Yang, H., Memon, S., Bao, X., et al.: Design and preparation of carbon based composite phase change material for energy piles. Materials **10**(4), 391 (2017)

Yavari, N., Tang, A., Pereira, J., Hassen, G.: Experimental study on the mechanical behavior of heat exchange pile using physical modeling. Acta Geotech. **9**(3), 385–398 (2014)

Ye, G., Ye, B.: Investigation of the overconsolidation and structural behavior of Shanghai clays by element testing and constitutive modeling. Undergr. Space **1**(1), 62–77 (2016)

Zhang, F., Ikariya, T.: A new model for unsaturated soil using skeleton and degree of saturation as state variables. Soil Found. **51**(1), 67–81 (2011)

Zhang, S., Leng, W., Zhang, F., Xiong, Y.L.: A simple thermo-elastoplastic model for geomaterials. Int. J. Plast **34**, 93–113 (2012)